

ENVIRONMENTAL CONTROL OF CLOUD-TO-GROUND LIGHTNING POLARITY IN SEVERE STORMS DURING IHOP

Lawrence D. Carey* and Kurt M. Buffalo
Texas A&M University, College Station, Texas

1. INTRODUCTION

The overwhelming majority of severe storms throughout the contiguous United States generate primarily (> 75%) negative ground flashes (so-called negative storms). However, a certain subset of severe storms produces an anomalously high (> 25%) percentage of positive ground flashes (so-called positive storms). The frequency of these “anomalous” positive storms varies regionally and seasonally. In some regions (e.g., central and northern plains) and months, these positive storms are common, representing 30% or more of all severe storms (Carey et al. 2003; Carey and Rutledge 2003).

MacGorman and Burgess (1994) noted that although many severe storms are dominated by negative cloud-to-ground (CG) flashes, severe storms constitute a small fraction of storms dominated by frequent negative CG flashes, but appear to constitute an overwhelming majority of storms dominated by frequent positive CG flashes. This possible relationship between positive CG flashes and severe storms suggests that real-time CG lightning flash data available to forecasters through the National Lightning Detection Network (NLDN) may be a useful nowcasting tool for severe weather (Carey et al. 2003). However, reliable nowcasting of severe weather based on positive CG production is not yet possible, since many severe storms are negative storms and not all positive storms are severe. Indeed, several studies have documented severe storms in which negative CGs were dominant (e.g., Curran and Rust 1992, Bluestein and MacGorman 1998). Thus, although there appears to be a relationship between increased positive CG production and severe storms, Branick and Doswell (1992) point out that the relationship is only a general one. As noted by MacGorman and Burgess (1994), “before forecasters can use positive cloud-to-ground lightning to help diagnose severe weather in these cases, research is needed to determine systematically under what conditions positive ground flashes occur in severe storms.”

Several past studies have noted that severe storms passing through similar mesoscale regions on a given day exhibit similar CG lightning behavior (Branick and Doswell 1992; MacGorman and Burgess 1994; Smith et al. 2000). This repeated observation led to the hypothesis that the local mesoscale environment

indirectly influences CG lightning polarity by directly controlling storm structure, dynamics, and microphysics, which in turn control storm electrification (e.g., MacGorman and Burgess 1994). According to one hypothesis, intense updrafts and associated high liquid water contents in positive storms lead to positive charging of graupel and hail via the non-inductive charging mechanism (e.g., Takahashi 1978; Saunders et al 1991), an enhanced lower positive charge, and increased frequency of positive CG lightning (e.g., MacGorman and Burgess 1994; Carey and Rutledge 1998; Gilmore and Wicker 2002). A handful of studies have explored the detailed relationship between the mesoscale environment and the CG lightning behavior of severe storms (Reap and MacGorman 1989; Curran and Rust 1992; Smith et al. 2000; Gilmore and Wicker 2002). Since it is difficult to obtain representative soundings, further study is warranted.

This study seeks to investigate the relationship between positive CG dominant storms and the immediate meteorological environment in which they occur, thereby providing further insight into why only some severe storms are dominated by positive CG flashes, and in particular, what conditions lead to this positive CG dominance. A determination of whether environmental conditions are systematically related to positive CG production by severe storms, and if so, what these conditions are, is a crucial step in determining the reliability of using NLDN real-time flash polarity data for nowcasting. Furthermore, determining the relationship between certain environmental conditions and positive severe storms will lead to an improved understanding of the cloud electrification mechanisms at work in these storms, which remains speculative at this time (e.g., MacGorman and Burgess 1994; Carey and Rutledge 1998; Smith et al. 2000; Williams 2001; Gilmore and Wicker 2002, Carey et al. 2003; Lang et al. 2004).

2. DATA AND METHODOLOGY

Using data from the International H₂O Project (IHOP), we explored the relationship between the local mesoscale environment and CG lightning behavior of severe storms. IHOP was conducted from 13 May to 25 June 2002 across the Southern Great Plains (Kansas, Oklahoma, and the Texas panhandle). The main goal of IHOP was to obtain more accurate and reliable measurements of moisture in the air, in an attempt to improve quantitative precipitation forecasts and increase understanding of convective initiation (Weckwerth et al. 2004). Thus, detailed measurements of the mesoscale

* *Corresponding author address:* Dr. Larry Carey, Dept. Atmospheric Sciences, Texas A&M University, College Station Texas 77843-3150; larry_carey@tamu.edu

Table 1. Classification and characterization of mesoscale regions within the IHOP-2002 domain according to the overall percentage of positive CG lightning (+CG %) produced by storms within them.

“POSITIVE MESOSCALE REGIONS” – Mesoscale regions containing >25% +CG lightning as produced by “positive storms” within them.					
Date	Time (UTC)	Latitude/ Longitude	+CG %	Storm Type(s)	Severe?
23 May 02	18-03	33° to 38°/ -103° to -100°	60.7	isolated supercells	YES
24 May 02	20-04	33.5° to 37°/ -101.5° to -98.5°	32.2	squall line (ordinary cells with several embedded supercells)	YES
15 June 02	18-03	32° to 39°/ -103° to -99°	43.4	multicell (ordinary and one supercell) evolving into squall line	YES
19 June 02	18-03	37° to 43°/ -103° to -97°	71.5	broken squall line of ordinary cells; isolated supercell	YES
“NEGATIVE MESOSCALE REGIONS” – Mesoscale regions containing ≤ 25% +CG lightning as produced by “negative storms” within them.					
Date	Time (UTC)	Latitude/ Longitude	+CG %	Storm Type(s)	Severe?
23 May 02	18-03	34° to 40°/ -100° to -94°	6.5	broad cluster of ordinary multicell convection	NO
24 May 02	20-04	32.5° to 38°/ -98.5° to -95°	7.5	broken squall line of ordinary cells	YES
4 June 02	12-01	33° to 40°/ -103° to -95°	9.2	squall line (ordinary cells with two supercells) evolving to LLTS MCS	YES
12 June 02	20-04	32° to 39°/ -103° to -95°	8.9	scattered supercells evolving into squall line	YES
15 June 02	18-03	32° to 39°/ -99° to -95.5	17.1	multicell (ordinary and one supercell) evolving into squall line	YES

environment in both the horizontal and vertical were obtained during IHOP. Although the focus of this study differs from that of IHOP, we can use the detailed measurements obtained during IHOP to help assess the relationship between the local mesoscale environment and positive severe storms. Of particular interest to this study is the multitude of environmental soundings taken during IHOP.

We have utilized these abundant environmental soundings taken during IHOP to document the relationship between mesoscale environment and dominant CG lightning polarity. We identified one non-severe negative (23 May), four severe negative (24 May; 4, 12, 15 June), and four severe positive (23, 24 May; 15, 19 June) storm systems on six different days during IHOP (Table 1).

To thoroughly characterize the local mesoscale environments of the nine storm systems, we analyzed soundings from several different platforms operating during IHOP. These sounding platforms include NWS upper-air sites, Atmospheric Radiation Measurement – Clouds and Radiation Testbed (ARM-CART) sites, the National Center for Atmospheric Research/Atmospheric Technology Division (NCAR/ATD) – Integrated Sounding System (ISS) facility, the National Severe Storms Laboratory (NSSL) Mobile Cross-chain LORAN Atmospheric Sounding System (MCLASS) facility, and NCAR/ATD MGLASS (mobile rawinsonde systems similar to CLASS systems, but containing GPS

technology) facilities, as well as dropsondes from the NCAR/ATD Learjet.

From hundreds of soundings taken by these platforms during IHOP, approximately fifty inflow proximity soundings that best represented the mesoscale environments of the nine storm systems (Table 1) were selected. As described in detail by Brooks et al. (1994), obtaining inflow proximity soundings that are truly representative of conditions experienced by a given storm is not a trivial task. Time and distance constraints must be applied to account for temporal and spatial variability in the environment, while other factors such as convective contamination and the presence of boundaries must also be considered when assessing the representativeness of a sounding. These issues were all accounted for in the compilation of this inflow proximity sounding data set.

The National Centers Advanced Weather Interactive Processing System Skew T Hodograph Analysis and Research Program (NSHARP) was used for sounding display and analysis. NSHARP includes a virtual temperature correction for thermodynamic calculations (e.g., Doswell and Rasmussen 1994). A mean-layer parcel (using mean temperature and dew point in the lowest 100 hPa) were used to calculate thermodynamic parameters, since a mean-layer parcel is likely more representative of the actual parcel associated with convective cloud development than is a surface-based parcel (Craven et al. 2002).

Table 2. Mean environmental properties of negative and positive mesoscale regions (see Table 1). The properties are grouped by the statistical significance level of the differences in means (Student's t-test).

Significance Level: 0.1%	Negative	Positive
Warm cloud depth (WCD=FL-LCL)	2949 m	1699 m
Lifting condensation level (LCL)	1121 m	2079 m
Mean mixing ratio in the lowest 100 mb	14.03 g kg ⁻¹	10.88 g kg ⁻¹
850–500 mb lapse rate	7.07 °C km ⁻¹	8.38 °C km ⁻¹
Wet-bulb zero (WBZ) height	3284 m	2868 m
Precipitable water in the surface to 400 mb layer	3.63 cm	2.72 cm
Significance Level: 1%		
0–3 km shear	10.70 m s ⁻¹	14.75 m s ⁻¹
Freezing level (FL)	4070 m	3777 m
CAPE between the LFC and -10°C level	397 J kg ⁻¹	199 J kg ⁻¹
Significance Level: 5%		
Convective Inhibition (CIN)	67 J kg ⁻¹	26 J kg ⁻¹
Equilibrium level (EL)	12545 m	11671 m
700–500 mb lapse rate	7.71 °C km ⁻¹	8.36 °C km ⁻¹
0–2 km storm-relative wind speed	6.97 m s ⁻¹	10.25 m s ⁻¹
Depth of free convective layer (EL–LFC)	9811 m	8604 m
CAPE between the -10°C and -40°C levels	957 J kg ⁻¹	1210 J kg ⁻¹
Normalized CAPE between the LFC and -40°C level	0.19 m s ⁻²	0.24 m s ⁻²
Significance Level: 10%		
0–3 km storm-relative environmental helicity (SREH)	72 m ² s ⁻²	163 m ² s ⁻²
Mid-level relative humidity (700–500 mb layer)	42%	32%
Mean relative humidity (through full depth of sounding)	37%	29%
Normalized CAPE (NCAPE from LFC to EL)	0.19 m s ⁻²	0.22 m s ⁻²
Normalized CAPE between -10°C and -40°C levels	0.24 m s ⁻²	0.29 m s ⁻²
Not significant at the 10% level		
CAPE (Convective Available Potential Energy, LFC to EL)	1924 J kg ⁻¹	1948 J kg ⁻¹
Lifted index (LI)	-6.92 °C	-6.11 °C
Level of Free Convection (LFC)	2682 m	2820 m
4–6 km storm-relative wind speed	10.66 m s ⁻¹	10.56 m s ⁻¹
6–10 km storm-relative wind speed	15.76 m s ⁻¹	15.12 m s ⁻¹
9–11 km storm-relative wind speed	22.77 m s ⁻¹	19.44 m s ⁻¹
0–2 km shear	8.17 m s ⁻¹	9.19 m s ⁻¹
0–6 km shear	17.72 m s ⁻¹	18.52 m s ⁻¹
Bulk Richardson number (BRN)	149	91
Energy helicity index (EHI using 0–3 km SREH)	0.8	1.99
Normalized CAPE between the LFC and -10°C level	0.13 m s ⁻²	0.11 m s ⁻²
CAPE between the LFC and -40°C level	1335 J kg ⁻¹	1405 J kg ⁻¹
Equivalent potential temperature (θ_e)	73.24 °C	71.95 °C

NSHARP computes and displays a multitude of environmental parameters, but special emphasis was placed on those variables that allowed us to test our hypothesis, which is succinctly stated here: *intense updrafts and associated high liquid water contents in positive storms lead to positive charging of graupel and hail in mixed-phase conditions via the non-inductive charging mechanism, an enhanced lower positive charge, and increased frequency of positive CG lightning.* For example, we emphasized those parameters that strongly influence storm organization, updraft intensity, and associated cloud water contents. A partial list of environmental parameters considered in this study can be found in Table 2. A more in-depth discussion of how these environmental parameters relate to our hypothesis will be presented when we discuss our results in Section 4.

The sounding data collected from NSHARP was analyzed to identify systematic differences in the local mesoscale environments of negative and positive storms. Using Microsoft Excel, statistical analysis of the parameters listed in Table 2 was conducted. Statistical characteristics of the variables such as means, medians, and percentiles were compared between positive and negative storms. Tests for differences of mean values (t-tests) were performed on the data to

identify significant differences between storm types. Different plotting schemes (e.g., histograms, scatter plots, etc.) were incorporated into the analysis to visually detect systematic differences between the two storm types.

3. RESULTS

Positive (negative) storms produced from 32% to 72% (7 to 17%) positive CG lightning in mesoscale regions over the IHOP domain (Table 1). All of the mesoscale regions were associated with severe weather except the negative region on 23 May 2002. There were no readily identifiable, systematic differences in storm organization or intensity within positive and negative mesoscale regions, as determined by visual inspection of regional radar composite imagery and Level II WSR-88D radar data. For example, there was no consistent relationship between cell type (supercell vs. ordinary multicell) and predominant CG polarity (positive or negative storms) (Table 1). However, positive mesoscale regions were somewhat more likely to support supercell convection than negative regions. Nonetheless, positive and negative storms were comprised of both supercell and ordinary multicellular convection as can be seen in Table 1.

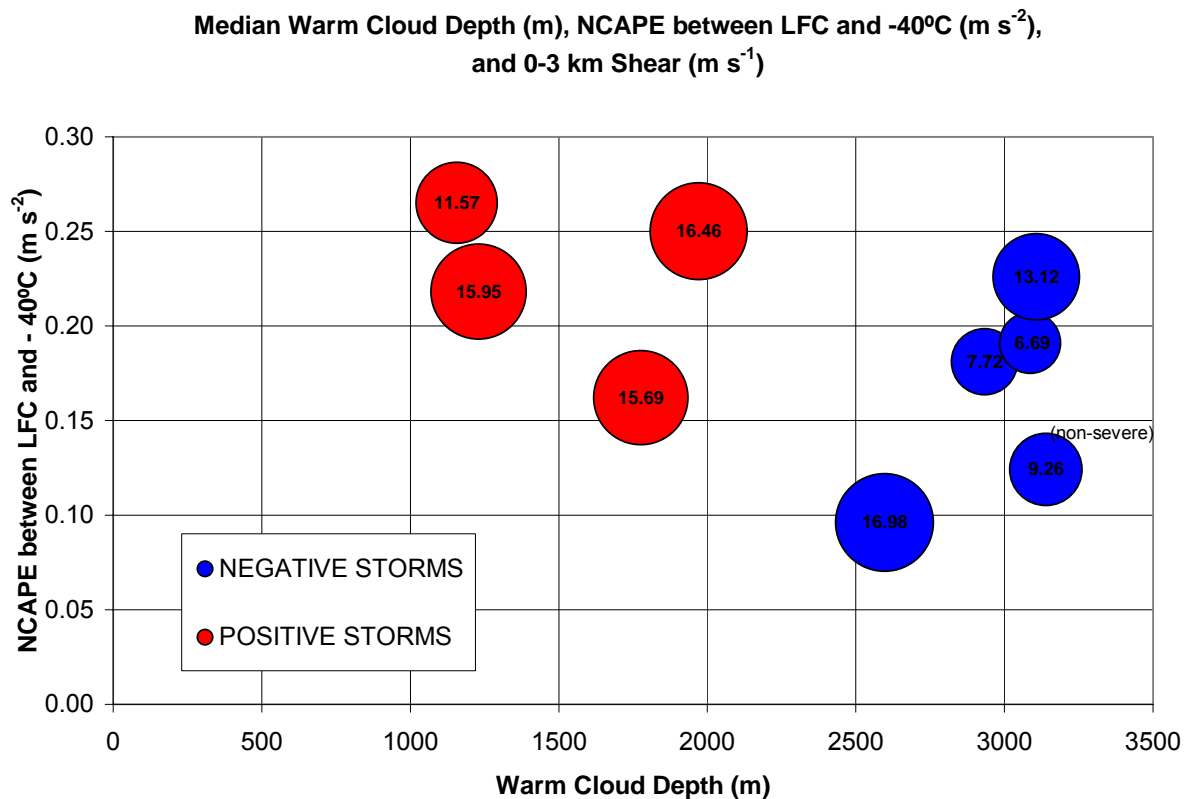


Figure 1. Scatter plot of the mean NCAPE (Normalized Convective Available Potential Energy, m s⁻²) between the level of free convection (LFC) and the height of the -40°C isotherm, which is the top of the mixed-phase zone, versus the mean warm cloud depth (m), which is defined as the height of the freezing level minus the lifting condensation level (LCL), in each of the nine mesoscale regions described in Table 1. The size of each bubble in the scatter plot is proportional to the magnitude (m s⁻¹) of the 0-3 km low-level shear; which is indicated by the label on each bubble.

The overall mean environmental parameters for negative and positive mesoscale regions are listed in Table 2 and ranked by significance level according to the Students' t-test (i.e., 0.1%, 1%, 5%, 10%, and not significant).

As noted in Knapp (1994), negative storms occurred in a moister environment as indicated by significantly higher mean precipitable water, low-level mixing ratio, mid-level (700-500 mb) relative humidity, and mean relative humidity through the depth of the sounding.

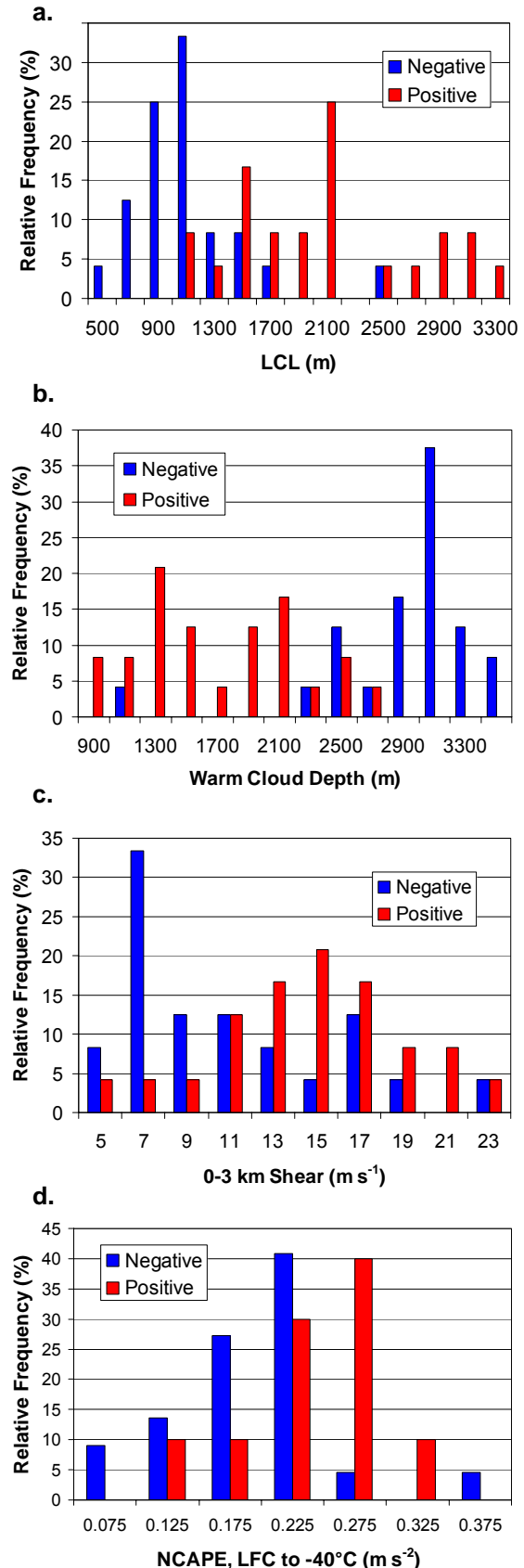
The positive mesoscale regions were characterized by a significantly higher mean lifting condensation level (LCL). Combined with a slightly lower freezing level (and wet-bulb zero height) in positive regions, the higher LCL resulted in a much more shallow mean warm cloud depth (i.e., depth of cloud at temperatures above 0°C) in positive mesoscale regions.

Mean lapse rates in the low-to-mid troposphere (850-500 mb and 700-500 mb) were higher in positive regions. The mean equilibrium level (EL) was higher in negative regions. So, despite little difference in the level of free convection (LFC) between negative and positive regions, the mean depth of the free convective layer (EL-LFC) was larger for negative regions.

Interestingly, there was no significant difference in the mean convective available potential energy (CAPE) and the lifted index (LI) for positive and negative regions. Similarly, the mean 0-6 km shear and the mean bulk Richardson number for each region were not significantly different. However, the mean convective inhibition (CIN) was higher for the negative regions.

As seen in Table 2, the mean CAPE in various layers was calculated for the positive and negative mesoscale regions. In general, there was more CAPE at warm temperatures (LFC to -10°C) in negative regions and more CAPE at colder temperatures (-10°C to -40°C) in positive regions. However, the mean NCAPE between the LFC and -10°C was not significantly different so the higher CAPE between LFC and -10°C in negative regions was associated with a deeper mean LFC to -10°C layer. The mean LFC to EL NCAPE and the mean -10°C to -40°C NCAPE were higher for positive mesoscale regions (but only significant to the 10% level). The most significant difference (5% level) in mean NCAPE between the two mesoscale regions was the higher mean value in the positive regions between the LFC and -40°C.

Figure 2. Relative frequency histograms of environmental parameters that characterize the mesoscale environment of negative and positive storms, including a) lifting condensation level (LCL, m), b) the warm cloud depth (m), which was defined here as the height of the environmental freezing level minus the LCL, c) the 0-3 km low-level shear ($m s^{-1}$), and d) the normalized convective available potential energy (NCAPE, $m s^{-2}$) from the level of free convection (LFC) to the height of the -40°C isotherm, which represents the top of the mixed-phase zone.



As shown in Table 2, the 0-3 km low-level shear and the 0-2 km storm-relative wind speed were significantly higher in positive mesoscale regions. Mean storm relative wind speed and mean wind shear defined at other levels were not significantly different between the positive and negative mesoscale regions. The mean 0-3 km storm-relative environmental helicity (SREH) was noticeably higher for positive mesoscale regions. Since the variance in the SREH was large, the difference was only significant at the 10% level. Since the mean CAPE was so similar for positive and negative regions, the energy helicity index (EHI) was also not significantly different between the two regions (at the 10% level).

To investigate differences between individual mesoscale regions, we calculated the mean warm cloud depth, NCAPE (LFC to -40°C), and 0-3 km shear separately for each mesoscale region listed in Table 1, as opposed to the overall positive and negative region means listed in Table 2, and depicted them together in a scatter plot (Figure 1). The two populations of mesoscale regions (i.e., positive and negative) are clearly distinct. As expected from Table 2, the large and systematic differences in warm cloud depth are responsible for much of the separation. The mean warm cloud depth for individual positive mesoscale regions ranged between 1000 and 2000 m while it exceeded 2500 m for negative mesoscale regions. Although the overall mean LFC to -40°C NCAPE and 0-3 km shear were significantly different between positive and negative mesoscale regions (Table 2), there was considerably more intra-category variability in the means for individual regions and much more overlap in means between individual positive and negative mesoscale regions. Although not shown, substitution of LCL for warm cloud depth yields a similar result as expected. The LCL clearly separates the population of negative and positive mesoscale regions. The mean LCL for individual positive (negative) mesoscale regions ranged from 1600 m to 3000 m (800 m to 1600 m).

To explore the entire range of variability of select environmental parameters, Figures 2a-d shows relative frequency histograms of LCL, warm cloud depth, 0-3 km shear, and NCAPE between the LFC and -40°C for all environmental soundings. The degree of separation between positive and negative mesoscale regions in the LCL (Figure 2a) and warm cloud depth (Figure 2b) of individual soundings was impressive. Although the populations were not completely distinct, there was very little overlap. However, it is important to note that high LCL and shallow warm cloud depth was not universally associated with positive storms as indicated by the outlier sounding that was launched in the vicinity of negative storms and was characterized by an LCL of about 2500 m and a warm cloud depth of about 1100 m. Comparatively speaking, there was much more overlap between the 0-3 km shear (Figure 2c) of individual positive and negative soundings but the modes of the two populations were distinct (15 m s^{-1} for positive and 7 m s^{-1} for negative with a secondary mode at 17 m s^{-1}). Similar results can be seen for the LFC to -40° NCAPE

in Figure 2d (0.275 m s^{-2} for positive and 0.225 m s^{-2} for negative).

4. DISCUSSION AND CONCLUSIONS

Using data from IHOP-2002, we have demonstrated clear, systematic differences between mesoscale regions associated with positive and negative storms. In particular, positive mesoscale regions are characterized by higher LCL, smaller warm cloud depth, larger CAPE from -10°C to -40°C , larger NCAPE from LFC to -40°C , larger 0-3 km shear, and larger 0-2 km storm-relative wind speed.

According to well known principals of dynamics and microphysics, each of these significant differences in the mesoscale environment would contribute to stronger updrafts and higher liquid water contents in the mixed-phase zone of positive storms (Bluestein 1993; Houze 1993). Larger NCAPE and 0-3 km shear in positive storms would result in stronger buoyancy and dynamic forcing of the updraft and hence larger updrafts in the mixed-phase zone (e.g., Weisman and Klemp 1982; Rotunno et al. 1988). Stronger 0-2 km storm-relative wind speed would result in stronger and more persistent low-level inflow of buoyant air into the updraft. Higher LCL, and hence cloud base height, is associated with increased horizontal diameter of the buoyant parcel or horizontal eddy size. The increased diameter of the updraft associated with the higher LCL would result in less entrainment, more efficient processing of CAPE, and ultimately stronger updrafts (e.g., Lucas et al. 1996; Williams and Stanfill 2002; Williams et al. 2004; Williams 2004). Smaller warm cloud depths would tend to suppress collision-coalescence processes (Williams et al. 2004; Williams 2004). All else being equal, warm rain processes (i.e., collision-coalescence) effectively reduces the amount of cloud water that is available in the mixed phase zone because of subsequent rainout or freezing of large rain drops. As a result, shallow warm cloud depths and the associated suppression of collision-coalescence would tend to increase the amount of supercooled cloud water available for non-inductive charging in the mixed phase zone (Williams et al. 2004; Williams 2004).

As a result, the IHOP results are consistent with the hypothesis that dominant positive CG lightning behavior in so-called positive storms is likely caused by a mesoscale environment that favors stronger updrafts and higher liquid water contents in the mixed phase zone, associated non-inductive positive charging of graupel and hail, and an enhanced positive charge at low-levels in the storms.

These observational results also have important implications for understanding the mesoscale environment of severe storms, lightning producing storms, and deep convection in general. As discussed in several recent papers (e.g., Lucas et al. 1994; 1996; Blanchard 1998; Williams and Stanfill 2002; McCaul et al. 2002; Zipser 2003; Williams et al. 2004), simple parcel theory and CAPE are often poor predictors of updraft strength and convective intensity in practice. For example, we found that CAPE, as diagnosed in

separate meaningful layers, and NCAPE were better correlated to the lightning behavior in severe storms. Furthermore, it appears that the LCL and its influence on updraft diameter and hence entrainment should be considered when evaluating the potential for intense updrafts and severe weather. Higher LCLs and hence cloud base heights may result in wider drafts, decreased entrainment, and increased efficiency with which CAPE is converted to kinetic energy.

5. REFERENCES

- Bluestein, H. B., 1993: *Observations and Theory of Weather Systems, Synoptic-Dynamic Meteorology in Midlatitudes*. Vol. II. Oxford University Press, 594 pp.
- Bluestein, H. B. and D. R. MacGorman, 1998: Evolution of cloud-to-ground lightning characteristics and storm structure in the Spearman, Texas, tornadic supercells of 31 May 1990. *Mon. Wea. Rev.*, **126**, 1451–1467.
- Branick, M. L., and C. A. Doswell III, 1992: An observation of the relationship between supercell structure and lightning ground-strike polarity. *Wea. Forecasting*, **7**, 143–149.
- Brooks, H. B., C. A. Doswell III, and J. Cooper, 1994: On the environments of tornadic and nontornadic mesocyclones. *Wea. Forecasting*, **9**, 606–618.
- Carey, L. D., and S. A. Rutledge, 1998: Electrical and multiparameter radar observations of a severe hailstorm. *J. Geophys. Res.*, **103**, 13 979–14 000.
- Carey, L. D., and S. A. Rutledge, 2003: Characteristics of cloud-to-ground lightning in severe and nonsevere storms over the central United States from 1989–1998. *J. Geophys. Res.*, **108**, 4483, doi:10.1029/2002JD002951.
- Carey, L. D., and S. A. Rutledge, and W. A. Petersen, 2003: The relationship between severe storm reports and cloud-to-ground lightning polarity in the contiguous United States from 1989 to 1998. *Mon. Wea. Rev.*, **131**, 1211–1228.
- Craven, J. P., R. E. Jewell, and H. E. Brooks, 2002: Comparison between observed convective cloud-base heights and lifting condensation level for two different lifted parcels. *Wea. Forecasting*, **17**, 885–890.
- Curran, E. B., and W. D. Rust, 1992: Positive ground flashes produced by low-precipitation thunderstorms in Oklahoma on 26 April 1984. *Mon. Wea. Rev.*, **120**, 544–553.
- Doswell, C. A., III, and E. N. Rasmussen, 1994: The effect of neglecting the virtual temperature correction on CAPE calculations. *Wea. Forecasting*, **9**, 619–623.
- Gilmore, M. S., and L. J. Wicker, 2002: Influences of the local environment on supercell cloud-to-ground lightning, radar characteristics, and severe weather on 2 June 1995. *Mon. Wea. Rev.*, **130**, 2349–2372.
- Knapp, D. I., 1994: Using cloud-to-ground lightning data to identify tornadic thunderstorm signatures and nowcast severe weather. *Natl. Wea. Dig.*, **19**, 35–42.
- Houze, R. A., Jr., 1993: *Cloud Dynamics*. Academic Press, 573 pp.
- Lang, T. L. and co-authors, 2004: The Severe Thunderstorm Electrification and Precipitation Study. *Bull. Amer. Meteorol. Soc.*, **85**, 1107–1126.
- Lucas, C., E. J. Zipser, and M. A. LeMone, 1994: Vertical velocity in oceanic convection off tropical Australia. *J. Atmos. Sci.*, **51**, 3183–3193.
- Lucas, C., E. J. Zipser, and M. A. LeMone, 1996: Reply. *J. Atmos. Sci.*, **53**, 1212–1214.
- MacGorman, D. R., and D. W. Burgess, 1994: Positive cloud-to-ground lightning in tornadic storms and hailstorms. *Mon. Wea. Rev.*, **122**, 1671–1697.
- Reap, R. M., and D. R. MacGorman, 1989: Cloud-to-ground lightning: Climatological characteristics and relationships to model fields, radar observations, and severe local storms. *Mon. Wea. Rev.*, **117**, 518–535.
- Rotunno, R., J. B. Klemp, M. L. Weisman, 1988: A theory for strong, long-lived squall lines, *J. Atmos. Sci.*, **42**, 271–292.
- Saunders, C. P. R., W. D. Keith, and R. P. Mitzeva, 1991: The effect of liquid water on thunderstorm charging. *J. Geophys. Res.*, **96**, 11 007–11 017.
- Smith, S. B., J. G. LaDue, and D. R. MacGorman, 2000: The relationship between cloud-to-ground lightning polarity and surface equivalent potential temperature during three tornadic outbreaks. *Mon. Wea. Rev.*, **128**, 3320–3328.
- Takahashi, T., 1978: Riming electrification as a charge generation mechanism in thunderstorms. *J. Atmos. Sci.*, **35**, 1536–1548.
- Weckwerth, T. M., and Coauthors, 2004: An overview of the International H₂O Project (IHOP_2002) and some preliminary highlights. *Bull. Amer. Meteor. Soc.*, **85**, 253–277.
- Weisman, M. L., and J. B. Klemp, 1982: The dependence of numerically simulated convective storms on vertical wind shear and buoyancy. *Mon. Wea. Rev.*, **110**, 504–520.
- Williams, E. R., 2001: The electrification of severe storms. *Severe Convective Storms, Meteor. Monogr.*, No. 50, Amer. Meteor. Soc., 527–561.
- Williams, E. R., 2004: The role of elevated cloud base height in the inverted electrical polarity of severe storms, this conference, paper 16B.4.
- Williams, E. R., and S. Stanfill, 2002: The physical origin of the land-ocean contrast in lightning activity. *C. R. Physique*, **3**, 1277–1292.
- Williams, E. R., V. Mushtak, D. Rosenfeld, S. Goodman, and D. Boccippio, 2004: Thermodynamic conditions favorable to superlative thunderstorm updraft, mixed phase microphysics and lightning flash rate. *J. Atmos. Res.*, in press.
- Zipser, E. J., 2003: Some views on “Hot Towers” after 50 years of tropical field programs and two years of TRMM data. *Cloud Systems, Hurricanes, and the Tropical Rainfall Measuring Mission (TRMM) – A Tribute to Dr. Joanne Simpson, Meteor. Monogr.*, No. 51, Amer. Meteor. Soc., 49–58.